

Conditional Deletion of *Rb* Causes Early Stage Prostate Cancer

Lisette A. Maddison,¹ Brent W. Sutherland,⁴ Roberto J. Barrios,² and Norman M. Greenberg^{1,3,4}

¹Department of Molecular and Cellular Biology, ²Department of Pathology, and ³Scott Department of Urology, Baylor College of Medicine, Houston, Texas; and ⁴Clinical Research Division, Fred Hutchinson Cancer Research Center, Seattle, Washington

ABSTRACT

Prostate cancer remains the second leading cause of cancer-related death for men in the United States. Mutations in tumor suppressor genes including retinoblastoma (*Rb*), *p53*, and *PTEN* have been linked to the development of prostate cancer in man and mouse models, and loss of heterozygosity of the *Rb* locus has been observed in up to 60% of clinical cases. In this study we demonstrate that conditional somatic deletion of even a single *Rb* allele in the epithelial cells of the mouse prostate causes focal hyperplasia, thereby establishing a causal relationship between *Rb* loss and development of early stage prostate cancer. As a consequence of *Rb* ablation we observed increased expression of E2F target genes and a concomitant increase in proliferation in the epithelial compartment. However, by 52 weeks of age these lesions had not become malignant and represent an early stage of the disease. Nevertheless, the multifocal nature of the phenotype in the mice closely resembled multifocality of clinical disease. Taken together, our data demonstrated that loss of pRB-mediated cell cycle control directly caused the initiation of proliferative prostate disease but was insufficient to cause malignancy. Establishment of this early initiation model will aid efforts to thoroughly characterize early prostate disease as well as the elucidation of molecular mechanisms that cooperate with *Rb* loss to facilitate progression and metastasis.

INTRODUCTION

Prostate cancer remains the second leading cause of cancer-related death of men in the United States. Nearly 30,000 men are predicted to die from prostate cancer in 2004, and an additional 230,000 men will likely be diagnosed with the disease (1). Despite the magnitude of these statistics, the underlying causes of prostate cancer remain elusive. Whereas several chromosomal regions have been implicated including 8p (2, 3), 10q (4), 13q (5–7), and 17p (8, 9), only a few of the candidate genes on these regions have been well characterized including *Nxk3* located on 8p (10), *PTEN* located on 10q (11), and *p53* located on 17p (12, 13).

The retinoblastoma tumor suppressor gene, *Rb*, located at 13q has also been associated with prostate cancer (14–16). Between 17% and 60% of prostate cancers demonstrate loss of heterozygosity of the *Rb* locus (15, 17–19), and both reduced expression of *Rb* mRNA (18) and pRB protein have been reported (15, 17). Although there has been no clear correlation between pRB loss and tumor stage or grade, several studies suggest that mutations in *Rb* can be early events in prostate cancer (5, 15, 20).

Because pRB maintains control of the G₁ to S-phase transition of the cell cycle primarily through interactions with the E2F family of transcription factors, mutations in *Rb* can promote the development of cancer by deregulating the expression of genes including *cyclin E*, *cyclin A*, and other components of the DNA replication machinery

(21). Whereas deregulation of the cyclin-dependent kinase inhibitor p16, D-type cyclins, and cdk4 molecules have been implicated in the majority of cancer types (22), mutations in *cyclin D* are relatively infrequent (23, 24) in prostate cancer, whereas p16 is often over expressed (25, 26) implying that direct abrogation of pRB function may be a major event. Moreover, several genetically engineered mouse models of prostate cancer in which the SV40 early genes are expressed under the temporal and spatial control of prostate specific promoters also implicate functional abrogation of pRB in prostate cancer (27–29). Unfortunately, it has been difficult to precisely determine the role of pRB loss in these models, because T antigen also targets p53, and the embryonic lethality of *Rb*^{−/−} mice (30–32) has hampered efforts to establish a causal relationship between pRB loss and the development of prostate cancer. Interestingly, although tissue recombinants generated with *Rb*^{−/−} epithelium have shown increased sensitivity to hormonal carcinogenesis *in vivo* (33), a direct causal relationship has yet to be established between pRB loss in the normally developed adult prostate and the emergence of sporadic somatic cancer.

To additionally investigate the potential causal relationship between *Rb* loss and prostate cancer we exploited a targeted conditional gene deletion (34). This system also provides an opportunity to investigate the tissue-specific consequence of gene loss. For example, whereas specific deletion of *Rb* in the pituitary gland has been observed to promote tumor development (35), similar deletion of *Rb* in the granular layer of the cerebellum was not observed to do so unless p53 was also deleted (36). On the basis of such rationale, we have used transgenic mice specifically expressing Cre recombinase in the prostate epithelium (37) to generate prostate-specific deletion of *Rb* and establish the causal relationship between RB loss and prostate cancer.

MATERIALS AND METHODS

Transgenic Mice. PB-Cre (8113-A) mice, heterozygous for the *PB-Cre* transgene, were maintained in a pure C57BL/6 background (Harlan Sprague Dawley, Inc., Indianapolis, IN). Mice homozygous for loxP modified *Rb* (*Rb*^{loxP}) obtained from Anton Berns (Netherlands Cancer Institute, Amsterdam, the Netherlands) were maintained in a pure 129S/V background. These mice were used to obtain PB-Cre⁺/*Rb*^{loxP/+} F1 animals. Male and female F1 animals were then intercrossed to obtain PB-Cre⁺/*Rb*^{loxP/loxP} and PB-Cre⁺/*Rb*^{loxP/+} mice. At least 5 mice were analyzed for each cohort. Control animals were composed of the PB-Cre[−]/*Rb*^{loxP/loxP}, PB-Cre[−]/*Rb*^{loxP/+}, PB-Cre[−]/*Rb*^{+/+}, or PB-Cre⁺/*Rb*^{+/+} genotypes. Littermates were used for all of the analyses. The PB-Cre⁺/*Rb*^{loxP/loxP} mice and control littermates were randomly assigned to cohorts and sacrificed at 12, 18, 36, and 52 weeks of age. When appropriate, animals were twice injected intraperitoneally with 10 mmol/L bromodeoxyuridine (BrdUrd) at 1 ml/100 g body weight once at 16 hours before sacrifice and once 2 hours before sacrifice. Approximately one-half of each prostate specimen was used for histological analysis, and remaining tissues were stored at −80°C and used for DNA, protein, or RNA analysis. All of the experiments were conducted using the highest standards for humane care in accordance with the NIH Guide for the Care and Use of Laboratory Animals.

PCR Amplification of Genomic DNA. Genomic DNA was isolated using standard protocols. Amplification of the *Rb* locus was performed using Rblox forward primer 5′ aactcaaggagacctg 3′ and Rblox reverse primer 5′ ggcgtggtccatcaatg 3′ at 1 μM/reaction with 1 mmol/L MgCl₂. Amplification was

Received 8/12/03; revised 6/22/04; accepted 6/25/04.

Grant support: National Cancer Institute Mouse Models of Human Cancer Consortium Grant UOICA84926 (N. Greenberg).

The costs of publication of this article were defrayed in part by the payment of page charges. This article must therefore be hereby marked *advertisement* in accordance with 18 U.S.C. Section 1734 solely to indicate this fact.

Note: L. Maddison is currently in the Vollum Institute, Oregon Health and Science University, Portland, OR 97239.

Requests for reprints: Norman Greenberg, Clinical Research Division, Fred Hutchinson Cancer Research Center, 1100 Fairview Avenue N. D4–197, Seattle, WA 98109-1024. Phone: 206-667-4433; Fax: 206-667-4930; E-mail: ngreenberg@fhcrc.org.

©2004 American Association for Cancer Research.

performed using 2.5 units of Taq polymerase (Promega) and annealing temperature of 60°C for 35 cycles.

Western Blot Analysis. Preparation of total cell lysates and Western blotting procedure were carried out as described elsewhere (38). A rabbit polyclonal antibody specific for the COOH-terminus of RB diluted 1:500 (C15; Santa Cruz Biotechnology, Santa Cruz, CA) or a monoclonal antibody specific for β -actin diluted 1:5000 (AC-74; Sigma) were used in the analysis. The resulting films were scanned and band intensity measured using NIH Image analysis software. All of the blots were performed in duplicate, and multiple samples were included in the analysis.

Histology and Immunohistochemistry. Fixation, sectioning, and immunohistochemical techniques were carried out as described previously (38). Histological criteria were based on a recommendation previously set forth by Park *et al.* (39) For this study antigen retrieval was performed with boiling in 10 mmol/L citric acid (pH 6.0) for 10 min. When appropriate slides were incubated with a rabbit polyclonal antibody specific for RB (Ab-6; Lab Vision, Fremont, CA) at a 1:50 dilution, p130/RB2 (Santa Cruz Biotechnology) at 1:500, p107 (Santa Cruz Biotechnology) at 1:500, or Ki67 (Novocastra, Newcastle, United Kingdom) at 1:1000. Incorporation of BrdUrd was detected using the BrdUrd labeling and detection kit II (Roche Diagnostics, Indianapolis, IN) using the manufacturer's recommendations. For analysis of proliferation or RB expression random slides were evaluated.

For each group, at least 30 random fields at $\times 40$ were counted to determine of total level of proliferation. Both BrdUrd-positive and total number of cells were counted with 11,594 total cells for PB-Cre⁺/Rb^{loxP/loxP} mice ($n = 9$), 3,178 total cells for PB-Cre⁺/Rb^{loxP/+} mice ($n = 4$), and 3,701 total cells for control littermates ($n = 5$). Proliferation in regions of hyperplasia was determined by counting the number of BrdUrd-positive and total cells within the lesion. For PB-Cre⁺/Rb^{loxP/loxP} mice, 75 lesions with a total of 5,930 cells were counted, 10 lesions with a total of 755 cells for PB-Cre⁺/Rb^{loxP/+} mice and 38 lesions with a total of 2,038 total cells for control littermates.

For analysis of RB expression within regions of hyperplasia, random slides were evaluated. Individual lesions were scored for high pRB expression where $>60\%$ of cells were RB positive, intermediate RB expression where between 30% and 60% of cells were RB positive, and low RB expression where $<30\%$ of the cells displayed RB immunoreactivity (39). Where indicated, regions of paraffin-embedded ventral prostate tissue of interest (5 μ m) containing at least 20% to $>50\%$ abnormal ductal epithelium from PB-Cre⁺/Rb^{loxP/loxP} and PB-Cre⁺/Rb^{loxP/+} mice were isolated by microdissection. Genomic DNA was extracted using the PicoPure DNA Extraction kit (Arcturus, Mountain View, CA) according to the manufacturer's instructions. PCR amplification of the Rb locus from DNA extracted from regions of interest from individual PB-Cre⁺/Rb^{loxP/loxP} and PB-Cre⁺/Rb^{loxP/+} mice was performed as described above using Rb1ox forward primer 5' aactcaaggagacctg 3' and Rb1ox reverse primer 5' ggcggtgcatcaatg 3'.

Statistical analyses were performed using Statview statistical analysis software (SAS Institute, Cary, NC) using analysis of variance (ANOVA) with Fisher's PLSD and Bonferroni/Dunn post-hoc tests or χ^2 analysis where appropriate.

Multiprobe RNase Protection Assay. RNA was isolated from dorsolateral and ventral prostate using Qiagen RNeasy Mini kit (Qiagen, Valencia, CA) according to the manufacturer's recommendations. RNA probes were prepared using *in vitro* transcription kit (BD PharMingen) and mouse cyclin multiprobe templates 1 and 2 (mCyc1, mCyc2 BD PharMingen). The RNase protection assay was carried out using 5 μ g of total RNA and the PharMingen RPA kit (BD PharMingen) according to the manufacturer's recommendations. Protected fragments were resolved on 5% acrylamide:urea gel and exposed to film (Kodak XAR). Resulting films were scanned and band intensity determined using NIH Image analysis software.

RESULTS

Deletion of loxP Modified Rb in Bigenic PB-Cre⁺/Rb^{loxP/loxP} Mice. To generate a conditional deletion of Rb specifically in prostate epithelial cells we crossed mice carrying a minimal probasin promoter-driven Cre recombinase transgene to mice that harbor loxP sites flanking exon 19 of Rb (Rb^{loxP}). Consistent with the restricted pattern of Cre recombinase expression in PB-Cre mice (37), recombination at

the Rb locus was observed exclusively in the ventral prostate lobe of both PB-Cre⁺/Rb^{loxP/+} and PB-Cre⁺/Rb^{loxP/loxP} mice (Fig. 1A). Recombination of the loxP modified Rb allele(s) was not observed in any other tissue examined including the dorsal and lateral lobes of the prostate or tissue isolated from PB-Cre⁻/Rb^{loxP/loxP} mice.

The Cre-mediated deletion of exon 19 of Rb leads to premature termination of pRB translation resulting in a truncated and functionally inactive protein (30, 35, 36). As shown in Fig. 1B, we detected decreased expression of full-length pRB protein in ventral prostate samples isolated from PB-Cre⁺/Rb^{loxP/loxP} mice. An average 1.3-fold decrease in pRB expression was observed in ventral prostate samples analyzed from multiple PB-Cre⁺/Rb^{loxP/loxP} mice. Consistent with the pattern of ventral prostate-specific Cre expression no significant change in expression of full-length pRB in the dorsolateral or anterior (data not shown) lobes of prostate glands of PB-Cre⁺/Rb^{loxP/loxP} mice were observed.

Prostate Phenotype in PB-Cre⁺/Rb^{loxP/loxP} Mice. The normal architecture of the mouse ventral prostate consists of ducts each lined by a single layer of flattened epithelial cells with small basal nuclei with each duct surrounded by a thin layer of smooth muscle cells (Fig. 2A). In the ventral prostate of PB-Cre⁺/Rb^{loxP/loxP} mice, we routinely observed focal areas of epithelial hyperplasia (Fig. 2, B–G). The pathological features ranged from restricted areas of hyperplasia (Fig. 2, C and E) where <100 cells were involved in a lesion to more extensive hyperplasia involving >100 cells that often extended into the ductal lumen (Fig. 2G). Mitotic figures (Fig. 2F) and apoptotic cells were clearly evident within the areas of hyperplasia. In addition, thickening of the smooth muscle layer was consistently observed to be associated with regions of epithelial hyperplasia (Fig. 2D). Although infrequent, focal regions of epithelial herniations were also apparent (Fig. 2G). We used periodic acid Schiff staining to demonstrate that the integrity of basement membranes and smooth muscle layers was compromised in these regions (Fig. 2, H and inset), and these herniations may represent preinvasive lesions. These features were consistently observed throughout several serial sections minimizing the likelihood that they represented artifacts of sectioning. More importantly, we were unable to detect similar lesions in control animals.

Prostate epithelial hyperplasias in PB-Cre⁺/Rb^{loxP/loxP} mice were apparent in limited areas as early as 12 weeks of age (Fig. 2B), an age where abnormal epithelium was infrequently observed in control

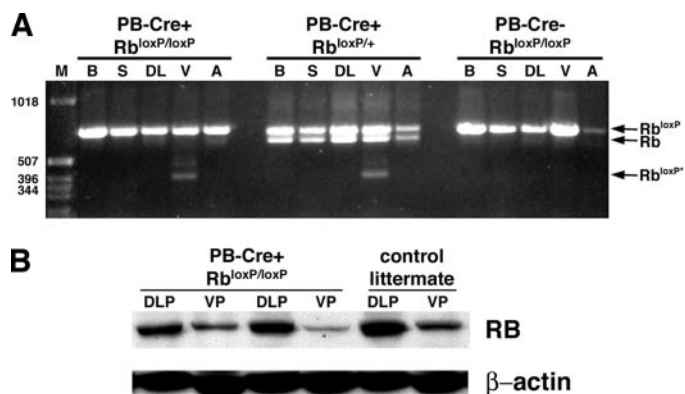


Fig. 1. Conditional deletion of retinoblastoma gene. A, PCR-based amplification of the loxP modified Rb allele(s). Genomic DNA isolated from bladder (B), seminal vesicle (SV), dorsolateral prostate (DL), ventral prostate (V), and anterior prostate (A) from mice of the indicated genotype amplified with primers annealing beyond the loxP sites flanking exon 19. Expected migration of PCR-amplified products indicating the wild-type Rb allele (Rb), loxP-modified Rb allele (Rb^{loxP}), and recombined Rb (Rb^{loxP/+}) is shown. B, Western blot analysis of RB expression. Protein isolated from dorsolateral prostate (DLP), ventral prostate (VP), and anterior prostate (AP) of mice of the indicated genotypes. The same membrane was probed with an antibody against the COOH terminus of RB or β -actin. These results are representative of data obtained from multiple mice.

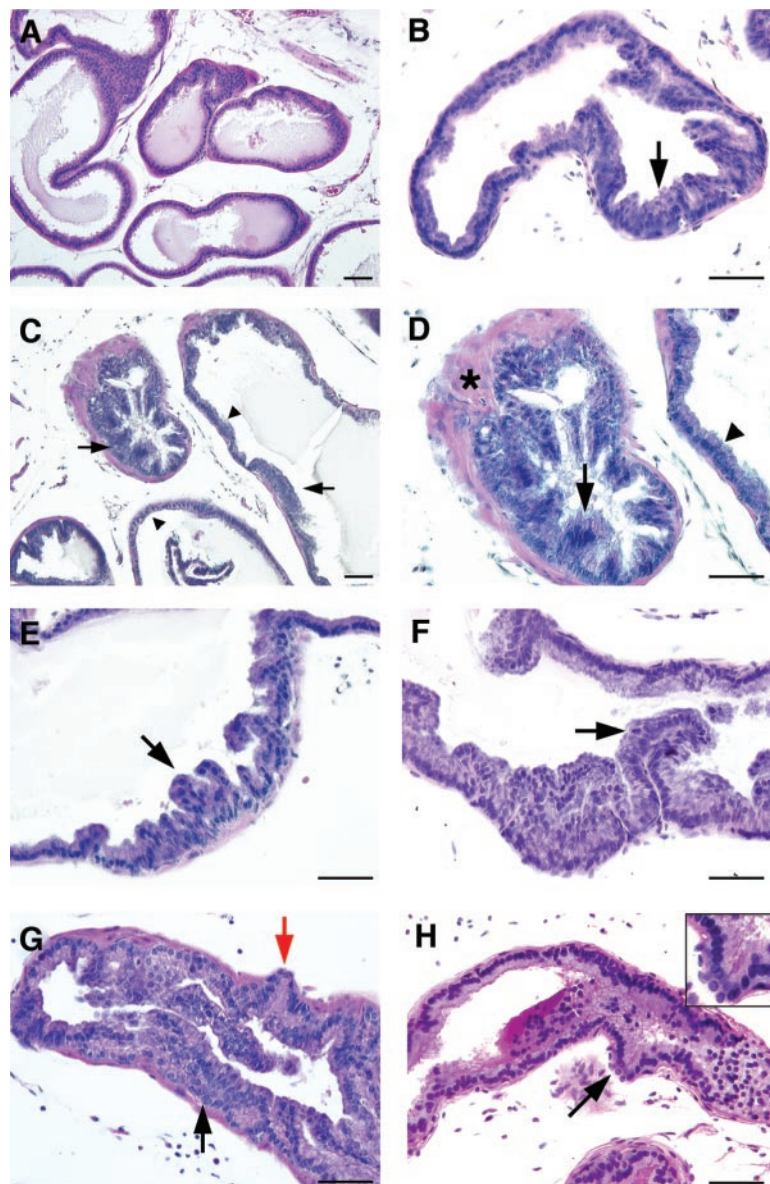


Fig. 2. Histological evaluation of the ventral prostate in PB-Cre⁺/Rb^{loxP/loxP} mice. Tissues were fixed, sectioned, and stained with hematoxylin and eosin. *A*, low-power micrograph of representative littermate control. *B*, representative 12-week-old PB-Cre⁺/Rb^{loxP/loxP} mouse. *Arrow* indicates region of hyperplasia. *C*, low-power image of PB-Cre⁺/Rb^{loxP/loxP} mouse, *arrowheads* indicate normal epithelium and *arrows* indicate areas of hyperplasia. *D* and *E*, high-power ($\times 400$ x) images of two 18-week-old PB-Cre⁺/Rb^{loxP/loxP} mice. *Arrows*, areas of epithelial hyperplasia; ***, area of stromal thickening. *F*, representative 36 week old PB-Cre⁺/Rb^{loxP/loxP} mouse. *Arrow*, mitotic figure. *g*) hematoxylin and eosin section of 18-week-old PB-Cre⁺/Rb^{loxP/loxP} mouse showing epithelial hyperplasia (*black arrow*) and epithelial herniation (*red arrow*). *H*, periodic acid Schiff-stained section from 18-week-old PB-Cre⁺/Rb^{loxP/loxP} mouse. Smooth muscle and basement membrane appear *bright pink*. *Arrow* and *inset*, region of epithelial herniation lacking these structures. Note that *G* and *H* are from two separate 18-week-old animals. *Bars*, 50 μ m.

animals (data not shown). By 18 weeks of age epithelial hyperplasia was routinely observed (Fig. 2) suggesting these lesions accumulated as a function of time. Hyperplasias were also evident in animals at 36 (Fig. 2*F*) and 52 weeks of age; however, no evidence of progression or development of nuclear atypia was observed suggesting that loss of pRB alone was insufficient to cause malignant transformation of the prostate epithelium.

As demonstrated in Fig. 2, the PB-Cre⁺/Rb^{loxP/loxP} mice demonstrated a predominantly focal phenotype. To fully assess the extent of epithelial abnormalities in 18-week mice, we quantified the areas of ventral prostate ducts that clearly deviated from the normal adult morphology (Fig. 2*A*). All of the slides were scored in a blinded manner. It should be noted that the mice were randomly assigned to cohorts to eliminate the possibility that any strain bias would exist for any particular genotype. Only a very low level of abnormal ductal epithelium (16.2%) was observed in control mice reflecting the intrinsic variation in the system. As shown in Table 1, a significant (ANOVA, $P < 0.05$) increase in the area of abnormal ductal epithelium was observed in both PB-Cre⁺/Rb^{loxP/loxP} mice (24.6%) and PB-Cre⁺/Rb^{loxP/+} mice (30%) suggesting that loss of a single *Rb*

allele was sufficient to promote hyperplasia. Importantly, we were unable to observe a significant increase in abnormal ductal epithelium in PB-Cre⁺/Rb^{+/+} mice ($18.4\% \pm 7.5\%$; t test $P = 0.147$) when compared with the other control genotypes ($14.8\% \pm 10.2\%$). Hence, expression of the Cre recombinase did not cause a nonspecific phenotype in our system, and the significant increase in abnormal epithelium was causally related to the *Rb* status.

To better characterize the range of phenotypes within a sample each duct was first determined to be either normal or abnormal by the criteria mentioned above. If abnormal, the percentage area of the atypical epithelium within the duct was then calculated. We estab-

Table 1 Area of ventral prostate with abnormal epithelium in 18-week-old mice

	Mice (n)	Sections (n)	Area of abnormal epithelium
PB-Cre ⁺ /Rb ^{loxP/loxP}	12	42	24.6% \pm 18.5*
PB-Cre ⁺ /Rb ^{loxP/+}	5	18	30.8% \pm 23.8†
Control genotypes	12	38	16.2% \pm 10.3

NOTE. All mice are littermates.

* ANOVA from control, $P = 0.04$.

† $P = 0.0015$.

Table 2 Percentage of individual ducts with abnormal epithelium in 18-week-old mice

	Mice (n)	Sections (n)	Ducts $\geq 20\%$ abnormal	Ducts $\geq 30\%$ abnormal	Ducts $\geq 50\%$ abnormal
PB-Cre ⁺ /Rb ^{loxP/loxP}	12	42	18.9% \pm 14.2*	11.2% \pm 9.5†	7.9% \pm 7.8‡
PB-Cre ⁺ /Rb ^{loxP/+}	5	18	18.7% \pm 12.4*	12.2% \pm 9.4†	6.6% \pm 6.5‡
Control genotypes	12	38	10.2% \pm 6.6	4.3% \pm 3.9	2.5% \pm 2.7

* ANOVA from control, $P < 0.01$.
 † ANOVA from control, $P < 0.02$.
 ‡ ANOVA from control, $P < 0.001$

lished three threshold levels for ducts with at least: (1) 20% abnormal epithelium, (2) 30% abnormal epithelium, or (3) 50% abnormal epithelium. All of the values were expressed as percentage of the total ducts in the sample. As described in Table 2 we observed more abnormal ducts in both 18-week-old PB-Cre⁺/Rb^{loxP/loxP} mice and PB-Cre⁺/Rb^{loxP/+} mice than in control mice at all of the threshold values.

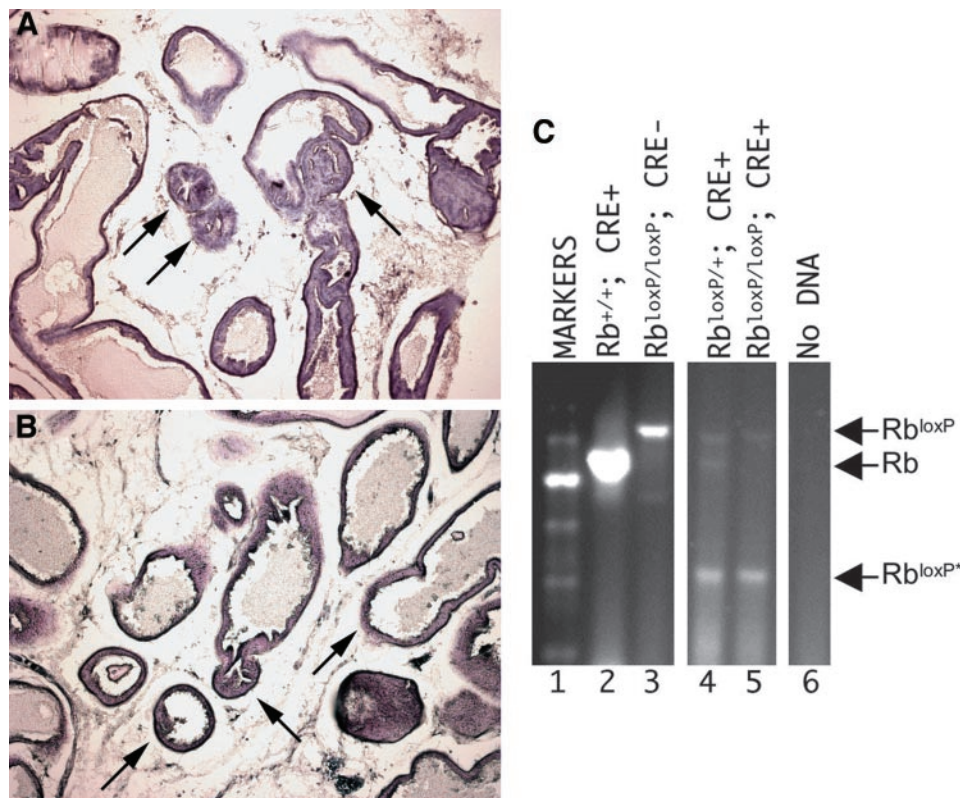
At 36 weeks of age, an increase in the percentage of ducts containing at least 50% abnormal epithelium was observed for both PB-Cre⁺/Rb^{loxP/loxP} mice (16.4%) and PB-Cre⁺/Rb^{loxP/+} mice (12.4%). However, an increase in abnormal epithelium in controls was also observed (10.7%), and no statistically significant difference in the level of abnormal epithelium at 36 weeks of age was observed. This observation additionally suggests that whereas loss of a single *Rb* allele may promote development of focal lesions at an early age, additional molecular events are required to facilitate malignant transformation of the prostate epithelium.

To directly correlate development of hyperplasia with loss of pRB, we performed tissue microdissection to demonstrate Cre-mediated recombination at the Rb^{loxP/+} and Rb^{loxP/loxP} alleles in PB-Cre⁺/Rb^{loxP/+} and PB-Cre⁺/Rb^{loxP/loxP} mice. As shown in Fig. 3, we clearly demonstrate that very nearly complete loss of one copy of *Rb* (Fig. 3A; PB-Cre⁺/Rb^{loxP/+}) correlated with a focal hyperplasia that was surprisingly no less or more severe than that observed after

virtually complete loss of both copies of *Rb* (Fig. 3B; Pb-Cre⁺/Rb^{loxP/loxP}) strongly supporting a causal relationship between *Rb* haploinsufficiency and prostate hyperplasia.

To additionally characterize the development of hyperplasia with loss of pRB, immunohistochemistry was used to examine the expression pattern of any full-length pRB protein remaining in prostate samples procured from PB-Cre⁺/Rb^{loxP/loxP} mice. We identified a normal pattern of nuclear RB expression in epithelial cells of the ventral prostate of control animals (Fig. 4A, panel a). A similar pattern was also observed in areas of PB-Cre⁺/Rb^{loxP/loxP} mice where the normal epithelial morphology was maintained (Fig. 4A, panels b–d). However, epithelial cells in areas of hyperplasia exhibited markedly decreased immunoreactivity for the pRB protein (Fig. 4A, panels b and c). Interestingly, epithelial cells along the basal surface of the ducts often displayed strong immunoreactivity, whereas hyperplastic epithelial cells were completely negative for pRB (Fig. 4A, panel b) or displayed a mix of pRB-positive and -negative cells (Fig. 4A, panel c). In addition, areas with abnormal but not hyperplastic ductal architecture demonstrated reduced expression of the full-length pRB protein in the epithelial compartments (Fig. 4A, panel d). In areas of hyperplasia from PB-Cre⁺/Rb^{loxP/loxP} mice, 29% (11 of 38) of lesions evaluated were observed to have low expression of RB, and 60% (23 of 38) displayed intermediate RB expression. In contrast, in control animals, no areas of hyperplasia were observed to display low ex-

Fig. 3. Loss of *Rb* in the ventral prostates of PB-Cre⁺/Rb^{loxP/loxP} and PB-Cre⁺/Rb^{loxP/+} mice. Paraffin thin sections of ventral prostate from an 18-week PB-Cre⁺/Rb^{loxP/loxP} mouse and a 36-week PB-Cre⁺/Rb^{loxP/+} mouse were dewaxed and lightly stained with hematoxylin and eosin. Routinely, genomic DNA was isolated from regions of interest containing 16–22 hyperplastic acini (arrows) from individual PB-Cre⁺/Rb^{loxP/loxP} (A) or PB-Cre⁺/Rb^{loxP/+} mice (B). Amplification of the *Rb* locus was performed as described above using Rblox forward and Rblox reverse primers (C) and fractionated on an agarose gel. Lane 1, molecular weight markers; Lane 2, amplified genomic tail DNA from a PB-Cre⁺/Rb^{loxP/+} mouse; Lane 3, amplified genomic tail DNA from a PB-Cre⁺/Rb^{loxP/loxP} mouse; Lane 4, amplified dissected tissue DNA from a PB-Cre⁺/Rb^{loxP/+} mouse; Lane 5, amplified dissected tissue DNA from a PB-Cre⁺/Rb^{loxP/loxP} mouse; Lane 6, control amplification with no DNA. Rb^{loxP}, amplified fragment representing the unrecombined Rb^{loxP} allele; Rb, amplified fragment representing the native *Rb* allele; Rb^{loxP*}, amplified fragment representing a recombined Rb^{loxP} allele.



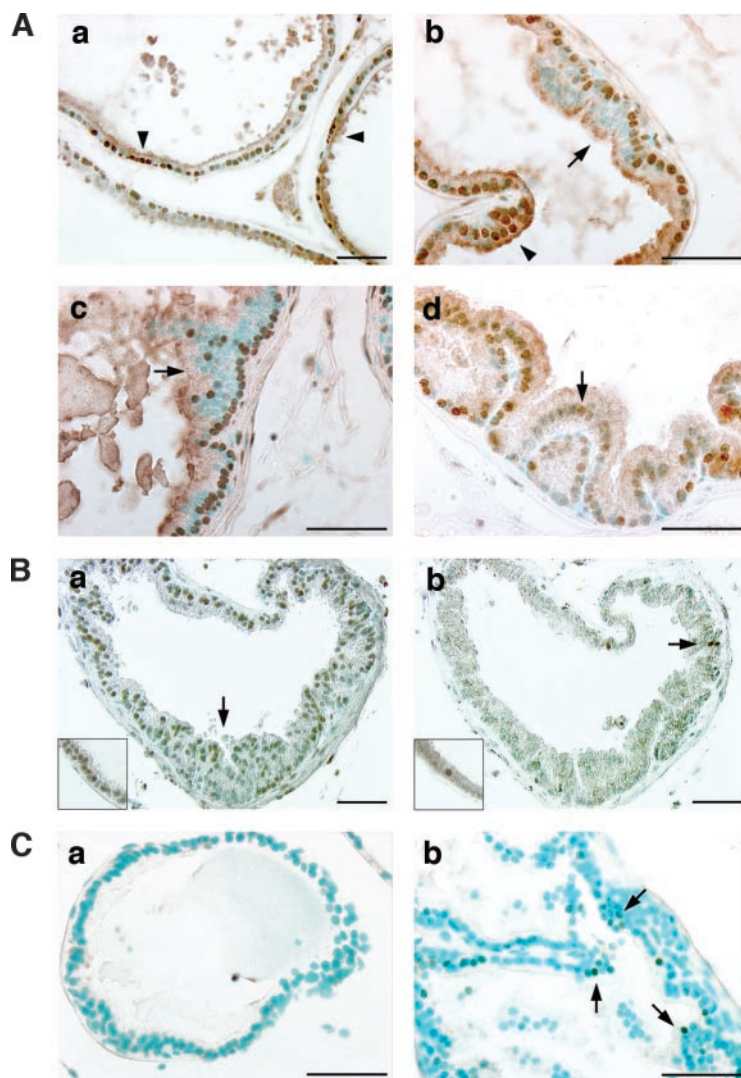


Fig. 4. Expression of RB, RB family members, and cyclin E. A, immunohistochemistry for full-length RB expression in 18-week-old control (panel a) or PB-Cre+/Rb^{loxP/loxP} mice showing hyperplasia with absent RB expression (panel b), mixed RB expression (panel c), abnormal ductal architecture with reduced RB expression (panel d). Arrowhead, normal nuclear RB expression; arrows, area of hyperplasia lacking expression of RB protein. B, p130/RB2 expression in PB-Cre+/Rb^{loxP/loxP} mouse; inset, section of control mouse (panel a). p107 expression in PB-Cre+/Rb^{loxP/loxP} mouse, inset, section of control mouse (panel b). C, cyclin E expression in 18 week control (panel a) and in hyperplasia from an 18-week PB-Cre+/Rb^{loxP/loxP} mouse (panel b). Bars, 50 μ m.

pression of RB (0 of 13), whereas 46% (6 of 13) displayed intermediate RB expression, and 54% displayed high RB expression. Furthermore, we observed a significant correlation between decreased pRB immunoreactivity and hyperplasia ($\chi^2 P < 0.02$). In general, our immunohistochemical data support our microdissection data that Rb inactivation correlates with hyperplasia.

We also performed an immunohistochemical analysis to account for the possibility that increased expression of p107 and p130/RB2 may have compensated for the loss of pRB. p130/RB2 was found to be highly expressed in the mouse prostate (Fig. 4B, panel a and inset); however, we were unable to detect a significant change in steady state expression of either p130/RB2 or p107 (Fig. 4B, panel b and inset) in PB-Cre+/Rb^{loxP/loxP} mice. It is unlikely, therefore, that any up-regulation of p107 or p130 occurred in these mice as a consequence of RB loss, in contrast to Rb germ line knockouts.

Consequences of Conditional RB Deletion. Because pRB is intimately associated with control of the cell cycle, we used BrdUrd incorporation as a measure of cellular proliferation in PB-Cre+/Rb^{loxP/loxP} mice. As shown in Fig. 5, a low basal level of proliferation was seen in the prostate glands of age-matched control littermate mice (Fig. 5A, panels a and b), whereas focal areas of epithelial hyperplasia in the ventral prostate of PB-Cre+/Rb^{loxP/loxP} mice often contained multiple proliferating cells (Fig. 5A, panels c-f). Overall proliferation rates measured by BrdUrd incorporation were found to increase from

1.0% in control animals ($n = 7$) to 1.2% in PB-Cre+/Rb^{loxP/+} mice ($n = 3$) and 1.5% in PB-Cre+/Rb^{loxP/loxP} mice ($n = 10$), but these findings were not statistically significant (ANOVA $P = 0.058$; Fig. 5B). In contrast, the level of proliferation specifically in areas of hyperplasia increased to 3.7% (ANOVA $P = 0.02$) in PB-Cre+/Rb^{loxP/+} mice ($n = 13$) and to 3.4% (ANOVA $P = 0.03$) in PB-Cre+/Rb^{loxP/loxP} mice ($n = 46$), whereas proliferation was only 2.3% in control mice (Fig. 5C). Similar results were observed using Ki67 expression as an independent measure of cellular proliferation (data not shown). These results demonstrate that a significant increase in proliferation specifically correlated to areas of hyperplasia in both PB-Cre+/Rb^{loxP/+} mice and PB-Cre+/Rb^{loxP/loxP} mice additionally strengthening the causal relationship between RB loss and development of hyperplasia.

Interactions between pRB protein and the E2F family of transcription factors maintain control over the G₁ to S transition of the cell cycle, and both cyclin E and cyclin A are known to be regulated by this pathway (21, 40). To characterize the consequence of conditional abrogation of pRB on steady state levels of cyclin mRNA, we performed an RNase protection assay on samples isolated from the prostate glands of PB-Cre+/Rb^{loxP/loxP} and control mice. As demonstrated in Fig. 6, we detected a low steady state level of cyclin E mRNA in the control mice and a slight but statistically significant (ANOVA $P = 0.027$) increase in steady state levels of cyclin E in

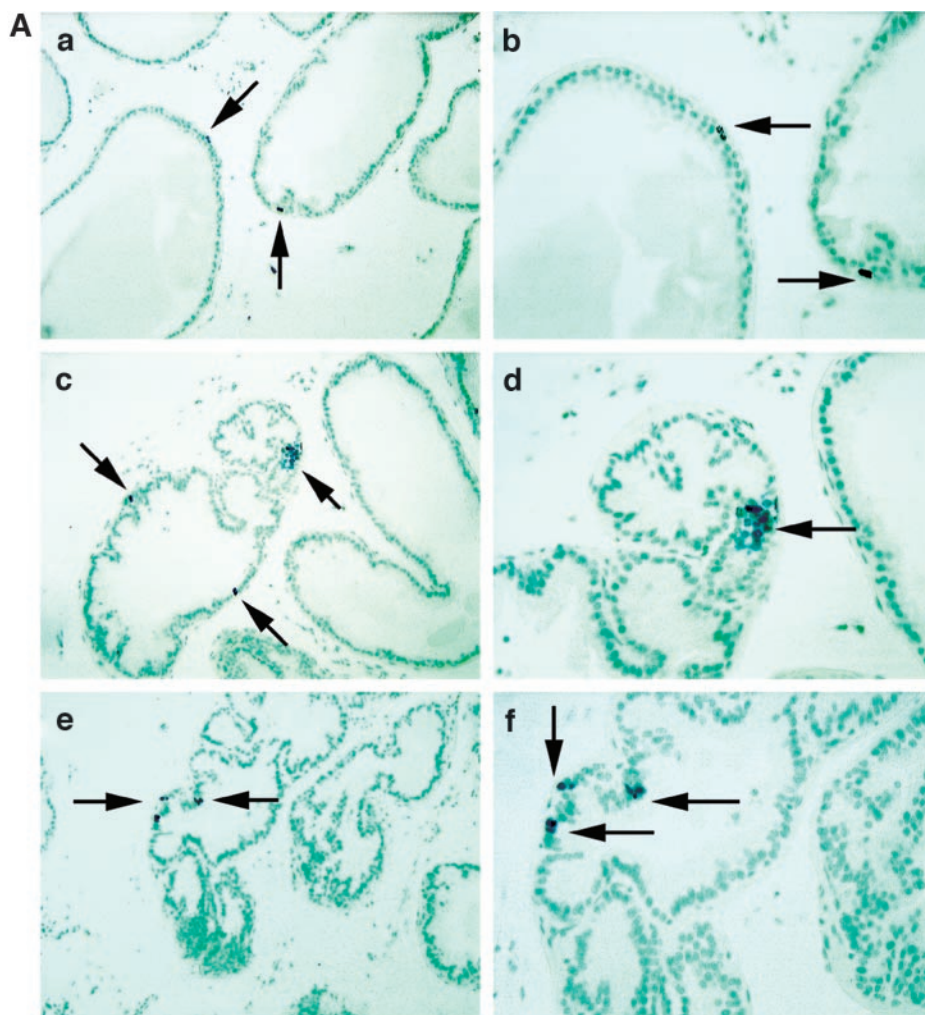
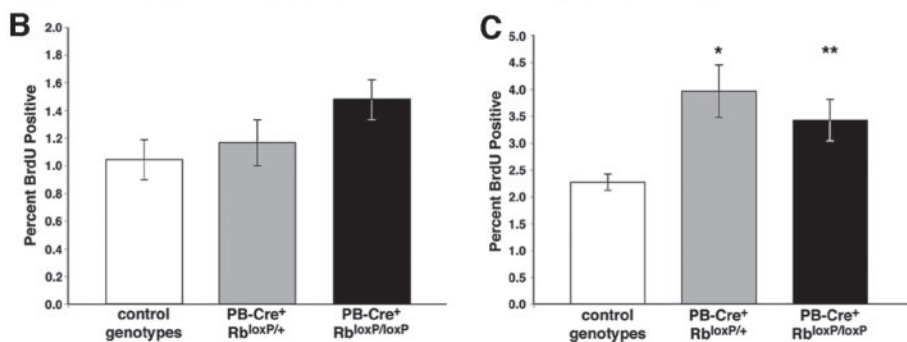


Fig. 5. Proliferation analysis of PB-Cre⁺/Rb^{loxP/loxP} mouse. A, immunohistochemistry for BrdUrd incorporation. Representative 18-week-old control at low (panel a) and high power magnification (panel b) or PB-Cre⁺/Rb^{loxP/loxP} mice at low (panels c and e) and high power magnification (panels d and f). Arrows, BrdUrd-positive cells. Bars, 50 μ m. B, overall proliferation index determined using at least 30 individual fields for each group. C, proliferation index specifically in areas of hyperplasia; bars, \pm SE.



ventral prostate samples from PB-Cre⁺/Rb^{loxP/loxP} mice. The increased level of *cyclin E* transcripts was consistent with loss of RB/E2F interactions in prostate epithelial cells. We also observed an increase in steady state levels of *cyclin D2* mRNA in the ventral prostates of PB-Cre⁺/Rb^{loxP/loxP} mice, although the increase in cyclin D2 expression was not statistically significant (ANOVA $P = 0.1$). Whereas cyclin D2 is not known to be regulated by pRB, the increase in cyclin D2 expression is consistent with an overall increase in proliferation as a consequence of conditional deletion of pRB. We additionally examined the expression of cyclin E at the cellular level in PB-Cre⁺/Rb^{loxP/loxP} mice. Expression of cyclin E was sporadic in the normal mouse prostate (Fig. 4C, panel a). However, in PB-Cre⁺/Rb^{loxP/loxP} mice expression of cyclin E was markedly increased in areas of hyperplasia (Fig. 4C, panel b). These observations provide

additional mechanistic evidence supporting a possible causal relationship between RB loss and expression of cyclin E associated with increased proliferation and initiation of prostate disease. A more thorough characterization of this relationship is currently underway.

DISCUSSION

Prostate cancer remains a significant health issue for aging men, and despite the advances in diagnosis the molecular mechanisms that directly control the initiation and progression of prostate cancer remain mostly uncharacterized. Although mutation of the retinoblastoma tumor suppressor gene has been associated with prostate cancer (6, 15–19) and may be an early event in this disease (5, 15, 20) a direct causal relationship between *Rb* loss and the development of prostate

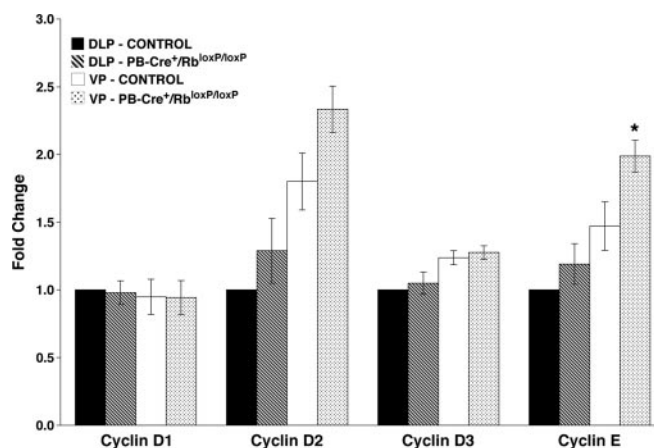


Fig. 6. Multiprobe RNase protection assay. Expression level of a spectrum of cyclin mRNA was analyzed using RNA isolated from dorsolateral prostate (DLP) or ventral prostate (VP) from either littermate controls or PB-Cre⁺/Rb^{loxP/loxP} mice. Cyclin mRNA levels were normalized to GAPDH and are expressed as fold change in expression relative to control DLP with the mean; bars, \pm SE. *, ANOVA $P = 0.027$.

cancer has not been established. In fact, our understanding of how individual genetic factors such as *Rb* loss contribute to the initiation and progression of the disease has been hampered by a paucity of animal models that appropriately mimic the natural history of this disease.

To directly test the hypothesis that there is a causal relationship between *Rb* loss and the initiation of prostate disease, we have applied a conditional system to abrogate pRB in the adult mouse prostate. Here, we now demonstrate that as early as 12 weeks of age, decreased expression of pRB protein correlates with epithelial cell hyperplasia and a corresponding increase in cellular proliferation and increase in expression of E2F regulated genes. Furthermore, this phenotype was observed even after deletion of a single *Rb* allele suggesting that haploinsufficiency of pRB can cause pathological changes in the prostate. Taken together, our data show that loss of pRB-mediated cell cycle control can initiate prostate disease and support the assertion that abrogation of *Rb* can be an early event in prostate cancer. This model is reflective of the nature of prostate cancer where only a subset of cells harbors a genetic alteration and recapitulates the multifocal nature of clinical disease. It is reasonable to propose, however, that abrogation of pRB in a larger percentage of prostate epithelial cells may lead to a more severe phenotype, similar to the dose dependency that has been reported for *PTEN* (40). The current model will also serve as a companion to other models exploiting tissue recombination (33) and the establishment of RB null prostate epithelial cells (41) to more fully address the molecular changes that cooperate with *Rb* loss.

Conditional models are the logical complement to more traditional germ-line knockout animals such as those established to analyze the role of Nkx3.1, p27, and Pten in the development and pathogenesis of prostate cancer (10, 42, 43). Because expression of Cre recombinase is temporally and spatially regulated (37, 44, 45), the mice can reach adulthood before the recombinase is expressed. Hence, we can examine the consequence of an engineered molecular lesion in a fashion that more closely reflects the spontaneous somatic events that likely occur in the majority of prostate cancer cases. Furthermore, conditional knockout models have an intrinsic cell-type specificity facilitating genetic perturbation in a defined cellular compartment in the context of an otherwise normal surrounding environment. An example of this advantage was reported between germ-line and conditional knockouts at the Nkx3.1 locus where the conditional knockouts (44) showed prostate lesions at an early age but in different locations than the germ-line knockouts (10).

It is important to highlight our observation that mice with abrogated pRB demonstrated rapid onset of hyperplasia without evidence of stochastic progression, an observation in reasonable agreement with data obtained from tissue recombination studies (33). However, the development of hyperplasia at a relatively early age was in contrast to previous reports describing mice expressing high levels of wild-type androgen receptor (46) or mice lacking either Nkx3.1 (10) or p27 (43). Because conditional pRB loss, like ablation of Nkx3.1 or p27 or enforced expression of wild-type androgen receptor, was insufficient to mediate development of malignant adenocarcinoma, other molecular events are likely required to facilitate malignant transformation. It may also be necessary to lose expression of p130/RB2 in order for the cells to exit the G₀ stage, and there is evidence to support this hypothesis. For example, it is known that differentiated cells express high levels of p130/RB2 (47), and we similarly observed robust expression of p130 in the mouse prostate. Because altered expression of p130/RB2 has been observed in human prostate cancer (48), it is therefore logical to propose that the combined loss of p130/RB2 and RB together may be required for malignant transformation. It should be possible now to test this hypothesis by deletion of both *Rb* and p130 through conditional targeted or other transgenic approaches such as enforced expression of the truncated SV40 early gene. Additionally, inactivation of pRB could also lead to p53-dependent apoptosis through p19^{ARF} (49). However, we were unable to observe an increased level of apoptosis in conditional *Rb* knockout prostate tissue (data not shown), although it should be noted that it is often difficult to visualize this event due to the temporal nature of apoptosis.

Detecting simple RB loss may become an important diagnostic tool to identify patients that are more likely to develop slow-growing, nonlethal cancer from those that may have accumulated additional mutations and require more aggressive therapy. Given our data, it will now be important to identify those molecular signaling pathways that can synergize with RB loss to support progression of localized prostate cancer of malignant disease. In fact, many genes have been suggested to be important in the development of prostate cancer including p53 (12, 13), Nkx3.1 (10), and PTEN (11), and each could synergize with the RB pathway in different ways. For example, inactivation of RB could trigger a p53-dependent pathway of apoptosis mediated through E2F and p19^{ARF} (49), and loss of p53 could allow the cells to accumulate additional genetic lesions, escape apoptosis, and obtain a distinct survival advantage. The application and extension of our system will be an important research tool to help elucidate pathways key in the development of prostate cancer and to assist in development and characterization of future diagnostic and therapeutic options.

ACKNOWLEDGMENTS

We would like to thank Dr. Anton Berns for providing the Rb^{loxP} mice, Dr. Paula Kaplan-Lefko and Dr. Wendy J. Huss for scientific input, Caroline Castile for animal husbandry, Diane Gentry for histology samples, and Alvenia Daniels for secretarial support.

REFERENCES

- Jemal A, Tiwari RC, Murray T, et al. Cancer statistics. *CA Cancer J Clin* 2004;54:8–29.
- He WW, Sciavolino PJ, Wing J, et al. A novel human prostate-specific, androgen-regulated homeobox gene (NKX3.1) that maps to 8p21, a region frequently deleted in prostate cancer. *Genomics* 1997;43:69–77.
- Voeller HJ, Augustus M, Madike V, Bova, GS, Carter KC, Gelmann EP. Coding region of NKX3.1, a prostate-specific homeobox gene on 8p21, is not mutated in human prostate cancers. *Cancer Res* 1997;57:4455–9. Erratum in: *Cancer Res* 1997; 57:5613.
- Feilolter HE, Nagai MA, Boag AH, Eng C, Mulligan LM. Analysis of PTEN and the 10q23 region in primary prostate carcinomas. *Oncogene* 1998;16:1743–8.

5. Li C, Larsson C, Futreal A, et al. Identification of two distinct deleted regions on chromosome 13 in prostate cancer. *Oncogene* 1998;16:481–7.
6. Dong JT, Boyd JC, Frierson HF Jr. Loss of heterozygosity at 13q14 and 13q21 in high grade, high stage prostate cancer. *Prostate* 2001;49:166–71.
7. Alers JC, Krijtenburg PJ, Vis AN, et al. Molecular cytogenetic analysis of prostatic adenocarcinomas from screening studies: early cancers may contain aggressive genetic features. *Am J Pathol* 2001;158:399–406.
8. Massenkeil G, Oberhuber H, Hailemariam S, et al. P53 mutations and loss of heterozygosity on chromosomes 8p, 16q, 17p, and 18q are confined to advanced prostate cancer. *Anticancer Res* 1994;14:2785–90.
9. Saric T, Brkanac Z, Troyer DA, et al. Genetic pattern of prostate cancer progression. *Int J Cancer* 1999;81:219–24.
10. Bhatia GR, Donjacour A, Scivolino P, et al. Roles for Nkx3.1 in prostate development and cancer. *Genes Dev* 1999;13:966–77.
11. Wang SI, Parsons R, Iltmann M. Homozygous deletion of the PTEN tumor suppressor gene in a subset of prostate adenocarcinomas. *Clin Cancer Res* 1998;4:811–5.
12. Henke RP, Kruger E, Ayhan N, Hubner D, Hammerer P, Hurland H. Immunohistochemical detection of p53 protein in human prostatic cancer. *J Urol* 1994;152:1297–301.
13. Voeller HJ, Sugars LY, Pretlow T, Gelmann EP. p53 oncogene mutations in human prostate cancer specimens. *J Urol* 1994;151:492–5.
14. Bookstein R, Rio P, Madreperla SA, et al. Promoter deletion and loss of retinoblastoma gene expression in human prostate carcinoma. *Proc Natl Acad Sci USA* 1990;87:7762–6.
15. Phillips SMA, Barton CM, Lee SJ, et al. Loss of the retinoblastoma susceptibility gene (RB1) is a frequent and early event in prostatic tumorigenesis. *Br J Cancer* 1994;70:1252–7.
16. Melamed J, Einhorn JM, Iltmann MM. Allelic loss on chromosome 13q in human prostate carcinoma. *Clin Cancer Res* 1997;3:1867–72.
17. Iltmann MM, Wiczorek R. Alterations of the retinoblastoma gene in clinically localized, stage B prostate adenocarcinomas. *Hum Pathol* 1996;27:28–34.
18. Tricoli JV, Gumerlock PH, Yao JL, et al. The Cooperative Prostate Network, N. C. I. Alterations of the retinoblastoma gene in human prostate adenocarcinoma. *Genes, Chromosomes & Cancer* 1996;15:108–14.
19. Brooks JD, Bova GS, Isaacs WB. Allelic loss of the retinoblastoma gene in primary human prostatic adenocarcinomas. *The Prostate* 1995;26:35–9.
20. Phillips SMA, Morton DG, Lee SJ, Wallace DMA, Neoptolemos JP. Loss of heterozygosity of the retinoblastoma and adenomatous polyposis susceptibility gene loci and in chromosomes 10p, 10q and 16q in human prostate cancer. *Br J Urol* 1994;73:62.
21. Dyson N. The regulation of E2F by pRB-family proteins. *Genes Dev* 1998;12:2245–62.
22. Sherr CJ. Cancer cell cycles. *Science* 1996;274:1672–7.
23. Drobnjak M, Osman I, Scher HI, Fazzari M, Cordon-Cardo C. Overexpression of cyclin D1 is associated with metastatic prostate cancer to bone. *Clin Cancer Res* 2000;6:1891–5.
24. Gumbiner LM, Gumerlock PH, Mack PC, et al. Overexpression of cyclin D1 is rare in human prostate carcinoma. *Prostate* 1999;38:40–5.
25. Henshall SM, Quinn DI, Lee CS, et al. Overexpression of the cell cycle inhibitor p16INK4A in high-grade prostatic intraepithelial neoplasia predicts early relapse in prostate cancer patients. *Clin Cancer Res* 2001;7:544–50.
26. Lee CT, Capodiceci P, Osman I, et al. Overexpression of the cyclin-dependent kinase inhibitor p16 is associated with tumor recurrence in human prostate cancer. *Clin Cancer Res* 1999;5:977–83.
27. Gingrich J, Barrios R, Foster B, Greenberg N. Pathologic progression of autochthonous prostate cancer in the TRAMP model. *Prostate Cancer and Prostatic Diseases* 1999;2:70–5.
28. Maroulakou I, Anver M, Garrett L, Green J. Prostate and mammary adenocarcinoma in transgenic mice carrying a rat C3(1) simian virus 40 large tumor antigen fusion gene. *Proc Natl Acad Sci USA* 1994;91:11236–40.
29. Kasper S, Sheppard PC, Yan Y, et al. Development, progression, and androgen-dependence of prostate tumors in probasin-large T antigen transgenic mice: a model for prostate cancer [corrected and republished article originally printed in *Lab Invest* 1998;Mar 78(3):319–33]. *Lab Invest* 1998;78:i-xv.
30. Clarke AR, Maandag ER, van Roon M, et al. Requirement for a functional Rb-1 gene in murine development. *Nature* 1992;359:328–30.
31. Lee EYP, Chang C, Hu N, et al. Mice deficient for Rb are nonviable and show defects in neurogenesis and haematopoiesis. *Nature* 1992;359:288–94.
32. Jacks T, Fazeli A, Schmitt EM, Bronson RT, Goodell MA, Weinberg RA. Effects of an Rb mutation in the mouse. *Nature* 1992;359:295–300.
33. Wang Y, Hayward SW, Donjacour AA, et al. Sex hormone-induced carcinogenesis in Rb-deficient prostate tissue. *Cancer Res* 2000;60:6008–17.
34. Nagy A. Cre recombinase: the universal reagent for genome tailoring. *Genesis* 2000;26:99–109.
35. Vooijs M, van der Valk M, te Riele H, Berns A. Flp-mediated tissue-specific inactivation of the retinoblastoma tumor suppressor gene in the mouse. *Oncogene* 1998;17:1–12.
36. Marino S, Vooijs M, van Der Gulden H, Jonkers J, Berns A. Induction of medulloblastomas in p53-null mutant mice by somatic inactivation of Rb in the external granular layer cells of the cerebellum. *Genes Dev* 2000;14:994–1004.
37. Maddison L, Nahm H, DeMayo F, Greenberg N. Prostate specific expression of Cre recombinase in transgenic mice. *Genesis* 2000;26:154–6.
38. Huss WJ, Hanrahan CF, Barrios RJ, Simons JW, Greenberg NM. Angiogenesis and prostate cancer: identification of a molecular progression switch. *Cancer Res* 2001;61:2736–43.
39. Park JH, Walls JE, Galvez JJ, et al. Prostatic intraepithelial neoplasia in genetically engineered mice. *Am J Pathol* 2002;161:727–35.
40. Trotman LC, Niki M, Dotan ZA, et al. Pten Dose Dictates Cancer Progression in the Prostate. *PLoS Biol* 2003;1:E59.
41. Day KC, McCabe MT, Zhao X, et al. Rescue of embryonic epithelium reveals that the homozygous deletion of the retinoblastoma gene confers growth factor independence and immortality but does not influence epithelial differentiation or tissue morphogenesis. *J Biol Chem* 2002;277:44475–84.
42. Podsypanina K, Ellenson LH, Nemes A, et al. Mutation of Pten/Mmac1 in mice causes neoplasia in multiple organ systems. *Proc Natl Acad Sci USA* 1999;96:1563–8.
43. Cordon-Cardo C, Koff A, Drobnjak M, et al. Distinct altered patterns of p27KIP1 gene expression in benign prostatic hyperplasia and prostatic carcinoma [see comments]. *J Natl Cancer Inst* 1998;90:1284–91.
44. Abdulkadir SA, Magee JA, Peters TJ, et al. Conditional loss of Nkx3.1 in adult mice induces prostatic intraepithelial neoplasia. *Mol Cell Biol* 2002;22:1495–503.
45. Wu J, Wu X, Huang J, Powell WC, Matusik RJ, Roy-Burman P. Generation of a prostate epithelial cell-specific Cre transgenic mouse model for tissue-specific gene ablation. In: *AACR: Mouse Models of Cancer*. La Jolla, California;2000;A-27.
46. Stanbrough M, Leav I, Kwan PW, Bublely GJ, Balk SP. Prostatic intraepithelial neoplasia in mice expressing an androgen receptor transgene in prostate epithelium. *Proc Natl Acad Sci USA* 2001;98:10823–8.
47. Classon M, Dyson N. p107 and p130: versatile proteins with interesting pockets. *Exp Cell Res* 2001;264:135–47.
48. Claudio PP, Zamparelli A, Garcia FU, et al. Expression of Cell-Cycle-regulated Proteins pRb2/p130, p107, p27(kip1), p53, mdm-2, and Ki-67 (MIB-1) in Prostatic Gland Adenocarcinoma. *Clin Cancer Res* 2002;8:1808–15.
49. Bates S, Phillips AC, Clark PA, et al. p14ARF links the tumour suppressors RB and p53. *Nature* 1998;395:124–5.

Cancer Research

The Journal of Cancer Research (1916–1930) | The American Journal of Cancer (1931–1940)

Conditional Deletion of *Rb* Causes Early Stage Prostate Cancer

Lisette A. Maddison, Brent W. Sutherland, Roberto J. Barrios, et al.

Cancer Res 2004;64:6018-6025.

Updated version Access the most recent version of this article at:
<http://cancerres.aacrjournals.org/content/64/17/6018>

Cited articles This article cites 47 articles, 20 of which you can access for free at:
<http://cancerres.aacrjournals.org/content/64/17/6018.full.html#ref-list-1>

Citing articles This article has been cited by 14 HighWire-hosted articles. Access the articles at:
</content/64/17/6018.full.html#related-urls>

E-mail alerts [Sign up to receive free email-alerts](#) related to this article or journal.

Reprints and Subscriptions To order reprints of this article or to subscribe to the journal, contact the AACR Publications Department at pubs@aacr.org.

Permissions To request permission to re-use all or part of this article, contact the AACR Publications Department at permissions@aacr.org.